Eurographics Symposium on Rendering - Experimental Ideas & Implementations (2016)
E. Eisemann and E. Fiume (Editors)

Subdivision Next-Event Estimation for Path-Traced Subsurface Scattering

David Koerner[1,2,3] Jan Novák[1] Peter Kutz[2] Ralf Habel[2] Wojciech Jarosz[1,4]

[1]Disney Research [2]Walt Disney Animation Studios [3]University of Stuttgart [4]Dartmouth College

Abstract

We present subdivision next-event estimation *(SNEE) for unbiased Monte Carlo simulation of subsurface scattering. Our technique is designed to sample high frequency illumination through geometrically complex interfaces with highly directional scattering lobes enclosing a scattering medium. This case is difficult to sample and a common source of image noise. We explore the idea of exploiting the degree of freedom given by path vertices within the interior medium to find two-bounce connections to the light that satisfy the law of refraction. SNEE first finds a surface point by tracing a probe ray and then performs a subdivision step to place an intermediate vertex within the medium according to the incoming light at the chosen surface point. Our subdivision construction ensures that the path will connect to the light while obeying Fermat's principle of least time. We discuss the details of our technique and demonstrate the benefits of integrating SNEE into a forward path tracer.*

Categories and Subject Descriptors (according to ACM CCS): I.3.7 [Computer Graphics]: Three-Dimensional Graphics and Realism—Raytracing

1. Introduction

Rendering scattering volumes that are enclosed by refractive boundaries—e.g. a marble statue, human tissue, milk, jewelry made of translucent materials—poses a great challenge for most rendering algorithms. A popular technique for reducing variance of Monte Carlo (MC) rendering is next event estimation (NEE), which estimates direct illumination by sampling a point on the emitter and testing its visibility by casting a shadow ray. To boost the efficiency of path tracing algorithms, NEE is often executed at every step of path construction.

The aforementioned examples present a challenge because their refractive boundary prevents the use of NEE for the interior part—the scattering medium. Since the basic NEE connects the point in the medium to the emitter using a straight line through the boundary, which clearly violates Fermat's principle of least time, it will always fail. Using NEE for the interior thus yields no benefit over the brute-force alternative, which finds incident light by shooting rays in random directions hoping that the refraction through the boundary will aim them towards an emitter. This approach suffers from high variance and causes prominent noise in the image.

Walter et al. [WZHB09] and Holzschuch [Hol15] extended the idea of NEE to work across refractive boundaries. They formulate it as a search problem seeking a two-segment connection (with the middle vertex on the boundary) that satisfies the law of refraction. Hanika et al. [HDF15] demonstrated how to seamlessly integrate such search-based NEE techniques into Monte Carlo estimators via importance sampling. The main drawback of these prior works is that the search for the boundary vertex may not succeed. Indeed, the more bumpy the interface is, the harder it becomes to exploit the geometric derivatives on which the surface search relies on.

We approach the problem of refracting through the boundary differently. Whenever the last path vertex before refraction is in the medium, we reverse the order of constructing the vertices by first fixing the boundary vertex, and then generating the last vertex in the medium such that, after the refraction, the path will continue towards an emitter. In other words, instead of walking over the surface, we search a point in the volume ensuring that the two-segment connection satisfies Fermat's principle. After reviewing related work in the next section, we tackle the following three non-trivial challenges:

- importance sampling of the boundary vertex from the second-to-last vertex in the medium,
- generation of the last vertex in the medium that satisfies the refraction constraint, and
- integration with standard path tracing via multiple importance sampling (MIS) [VG95].

2. Previous Work

Generating paths that connect light sources to the sensor is a popular approach to simulating light transport. Originally proposed by Kajiya [Kaj86] and Immel et al. [ICG86], it was later improved

© 2016 The Author(s)
This is the author's version of the work. It is posted here for your personal use, not for redistribution. The definitive version is available at http://diglib.eg.org/.

by bidirectional construction [LW93, VG94] and metropolis sampling [VG97], and refined by many others to address specific rendering challenges. Notably, it has been shown that the problem of generating a valid connection through a refractive boundary can be sidestepped using density estimation approaches [Jen96, SZLG10, JNSJ11]. While robust, these are at best only consistent, consume memory, and require fairly involved techniques for distributing photons effectively [HJ11, VKv*14]. Despite these advances, some industries, such as animation and VFX, still value the simplicity and predictability of standard path tracing, which can be better extended to handle their specific problems.

NEE in Volumes. Our technique focuses on one such problem—rendering of scattering translucent objects—and shares similarities with the previously introduced techniques for NEE. The concept of scoring a weighted contribution at each vertex along a path in a medium is well researched in transport literature [KC77], and extends beyond connecting the path vertex to the source (or sensor) using a straight line—also known as the uncollided flux estimator (UCF) [Kal63]. For instance, the once-collided flux estimator [SK71] constructs two-segment connections using a density, which cancels the $1/r^2$ singularity that causes UCF to suffer from unbounded variance. This idea has been also introduced into graphics [KF12] and further extended to three-segment connections [GKH*13] to further reduce variance. A generalization of the aforementioned techniques is the adjoint-quantity based, zero-variance integration scheme [Dwi82, Kd14]. All the aforementioned techniques are concerned with transport only *inside* a volume, which may have a boundary. Our goal, in contrast, is to perform three-segment connections *across* the refractive boundary.

NEE Crossing a Boundary. Efficient handling of NEE across a refractive boundary has been addressed by Walter et al. [WZHB09] who propose searching for a point on the boundary, which will refract light from the emitter to the shading point, using a position–normal tree over the geometry and the Newton–Raphson iterative method. Holzschuch [Hol15] reverses the order of the loops and intersects the ray with refracted triangular prisms in the volume. Hanika et al. [HDF15] propose a more lightweight method, which leverages manifold exploration [JM12] to support refraction through multiple layers, and demonstrate how to integrate their approach into a unidirectional path tracer using MIS. The main drawback of these techniques is that they do not handle detailed or displaced surfaces well, since the iterative search, which needs to be constrained to the surface, can fail to find a solution. We observe that the refraction constraint can be trivially satisfied when increasing the dimensionality of the search space. As such, instead of performing a search over the 2D surface, we carefully place the last vertex in the 3D interior medium: we search for a position inside the volume that satisfies the law of refraction for a path passing through a previously chosen surface point.

3. Problem Statement

In order to simulate subsurface scattering, standard forward path tracing will, upon hitting the translucent object, refract through the dielectric boundary at the entry point x_0, build a path trough the interior, and exit the object by again refracting across the boundary at x_k (see Figure 1, left).

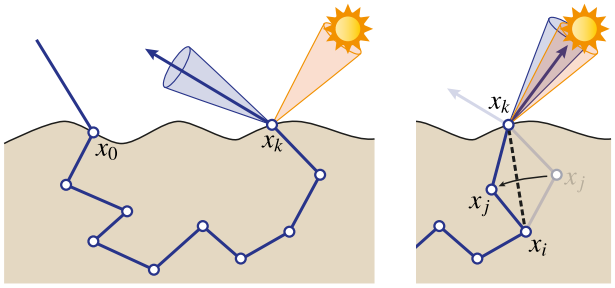

Figure 1: *Forward path tracing often struggles connecting to light sources through refractive boundaries (left). Our subdivision NEE overcomes this by ensuring that the last vertex in the medium x_j can be connected to the light using a two-segment shadow ray.*

The interactions with the medium are governed by the radiative transfer equation (RTE) [Cha60], which is parameterized by the absorption, scattering, and extinction coefficients, $\sigma_a(x)$, $\sigma_s(x)$, and $\sigma_t(x) = \sigma_a(x) + \sigma_s(x)$, respectively, and the phase function f_p, characterizing the directional distribution of scattered light; see e.g. PBRT [PH10] for details. The subsurface path $\mathbf{x}_k = (x_0 \ldots x_k)$ is constructed incrementally by sampling directions and distances to succeeding collision points (vertices). The probability density function (PDF) of a new vertex x_i depends on the sampling technique and is conditioned on the current path. The product of this conditional probability and the probability of the current path gives the PDF of the new path: $p(x_0 \ldots x_i) = p(x_i | x_0 \ldots x_{i-1}) p(x_0 \ldots x_{i-1})$.

The interactions with the boundary are handled by sampling the bidirectional scattering distribution function (BSDF) f_s, and result in either internal reflection or refraction with appropriate weighting of the path throughput. In the case of a smooth dielectric boundary, the reflection and refraction are deterministic, constrained by Fermat's principle of least time, with the latter described by Snell's law. When the boundary is rough, the outgoing direction is importance sampled using the BSDF, but most implementations also execute NEE to maximize the chances of directly connecting to an emitter; the two strategies are typically combined using MIS.

Unfortunately, the benefits of using NEE, as described above, diminish as the smoothness of the dielectric boundary increases. In fact, executing NEE on perfectly smooth boundaries is wasteful, because directions towards the sampled emitter will not satisfy Snell's law of refraction. The situation becomes even worse when the emitters subtend only a small solid angle. In such cases the likelihood that the lobe of refracted directions will sufficiently overlap with the cone confining the light is very small. The problem can be somewhat mitigated by mollifying one of the two high frequency functions, e.g. the BSDF [KD13], but this introduces bias and lower convergence rate than that of path tracing, even if the estimation is formulated consistently. Performing NEE at the interior vertices $x_1 \ldots x_{k-1}$ is potentially beneficial, since the volume's phase function will often be more isotropic than the boundary's BSDF, but such NEE connections face the challenge of properly refracting through the boundary.

© 2016 The Author(s)
For personal use only. The definitive version is available at http://diglib.eg.org/.

4. Subdivision Next-Event Estimation

In this section, we describe a new, two-bounce next-event estimation that allows collecting refracted light from emitters at vertices of a subsurface path. The goal is to enforce a multi-segment shadow ray to exit the boundary in a direction towards the emitter. Our approach is inspired by the idea of Brownian bridges [RY94] that construct long paths by subdividing path segments, hence the name *subdivision* NEE (SNEE).

The incident illumination arriving from direction ω_i at path vertex x_i, that we aim to estimate using SNEE, is described by the following equation:

$$L(x_i,\omega_i) = \int_{\mathcal{V}} S_{ij} \int_{\mathcal{S}} f_{ijk}\, S_{jk} \int_{\mathcal{E}} f_{jkl}\, S_{jk}\, L_e(x_l,-\omega_k)\,\mathrm{d}x_l \mathrm{d}x_k \mathrm{d}x_j, \quad (1)$$

where $\mathcal{V}$ and $\mathcal{S}$ are the interior volume and boundary surface of the translucent object, respectively, $\mathcal{E}$ is the union of emissive volumes and surfaces, and S and f are the segment and vertex throughputs defined as:

$$S_{ij} = T(x_i,x_j)\,V(x_i,x_j)\,\frac{c(x_i,x_j)\,c(x_j,x_i)}{\|x_i-x_j\|^2} \quad (2)$$

$$f_{ijk} = \begin{cases} f_p(x_i,x_j,x_k)\,\sigma_s(x_j), & \text{if } x_j \in \mathcal{V}, \\ f_s(x_i,x_j,x_k), & \text{otherwise,} \end{cases} \quad (3)$$

where $T(x_i,x_j)$ and $V(x_i,x_j)$ quantify the transmittance and visibility between x_i and x_j. The fraction in Equation (2) is the *geometry* term with $c(x_i,x_j) = 1$ if $x_i \in \mathcal{V}$, and $c(x_i,x_j) = \left|n(x_i)\cdot\omega_{ij}\right|$ otherwise, where $n(x)$ is the surface normal at x_i, and ω_{ij} is direction from x_i towards x_j.

When estimating Equation (1) using forward path tracing, the three-segment path $x_ix_jx_kx_l$ is constructed in-order. The main idea of SNEE is to reverse the order and sample x_j as the last one, such that the two-segment connection $x_jx_kx_l$ obeys the law of refraction. Given a path prefix $\mathbf{x}_i = (x_0 \ldots x_i)$, we first sample a boundary vertex x_k and then *subdivide* the connection x_ix_k by constructing an intermediate volume vertex x_j. The probability of constructing the path in this order reads:

$$p(\mathbf{x}_ix_jx_k) = p(\mathbf{x}_i)\,p(x_k|\mathbf{x}_i)\,p(x_j|\mathbf{x}_ix_k). \quad (4)$$

We detail the individual steps of the construction in following subsections.

4.1. Sampling Boundary Vertex x_k.

There are many options for choosing the boundary vertex x_k, through which the the subsurface path will refract. It is important to note, however, that the density $p(x_k|\mathbf{x}_i)$ needs to be easy to evaluate. We draw x_k from a PDF that is based on the geometry term of direct connections to the surface:

$$p(x_k|\mathbf{x}_i) = \frac{c(x_k,x_i)}{\|x_k-x_i\|^2}, \quad (5)$$

which can be easily realized by sampling a random direction and setting x_k to the first intersection with the boundary. As such, the density for drawing x_k is proportional to the geometry term of connecting to the boundary *directly*. However, an ideal density in this case would be proportional to the product of geometry terms along the two subdivision segments, where which the path throughput is to be evaluated. Unfortunately, this turns out to be nontrivial; we discuss the difficulties in Section 7, and we thus opt for the easily realizable density in Equation 5.

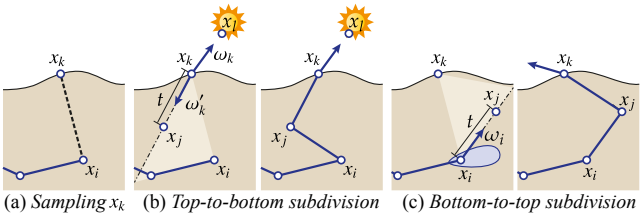

(a) *Sampling* x_k (b) *Top-to-bottom subdivision* (c) *Bottom-to-top subdivision*

Figure 2: *After sampling x_k (a), we combine two strategies for creating x_j: one addressing directional light sources (b), and one for anisotropic phase functions (c).*

4.2. Subdividing Segment x_ix_k

With the boundary point x_k known, we proceed by subdividing segment x_ix_k to construct the intermediate vertex x_j. The density for drawing x_j should ideally minimize the variance of estimating the light that arrives at x_i upon refracting through x_k and scattering inside the interior volume. To this end, we propose two complementary strategies: one for handling strongly directional light sources, and one for media with highly anisotropic phase functions.

Top-to-Bottom Subdivision. If the translucent object is illuminated by a (delta) directional light source—sampled to produce an emitted light ray traveling in direction $-\omega_k$—a good strategy is to constrain x_j to lie on the refracted ray (x_k,ω'_k); see Figure 2 for illustration. This ensures that, when the subsurface path exits the object, it will continue in the direction towards the emitter. Note that when the boundary is rough, the refracted direction ω'_k will be sampled using the BSDF. Having vertex x_i and ray (x_k,ω'_k), we sample the distance t along the ray using transmittance sampling [RSK08] with density $p_{\mathrm{tr}}(t)$ or equiangular sampling [KF12] $p_{\mathrm{eq}}(t)$, and combine both strategies using MIS. The conditional PDF of x_j reads:

$$p_{\downarrow}(x_j|\mathbf{x}_ix_k) = p_{\mathrm{light}}(-\omega_k)\,p_{\mathrm{bsdf}}(\omega'_k)\,\mathrm{MIS}\left[p_{\mathrm{tr}}(t),p_{\mathrm{eq}}(t)\right]; \quad (6)$$

we mark the PDF with $\downarrow$ to emphasize that the subdivision is constructed from the boundary vertex (top) towards the interior vertex (bottom). Please note that all PDFs on the right-hand side of Equation (6) are conditional; we omit this in the notation for brevity.

Bottom-to-Top Subdivision. When the interior medium has a highly anisotropic phase function f_p, path samples constructed using $p_{\downarrow}$ will suffer from high variance; f_p is not considered when building the path. To address this, we allow building the subdivision bottom to top: we first sample a direction ω_i, either by phase function importance sampling or using the $\mathcal{U}_2$ strategy proposed by Georgiev et al. [GKH*13], and then sample distance t, again using the transmittance or equiangular sampling. The PDF of such bottom-to-top construction reads:

$$p_{\uparrow}(x_j|\mathbf{x}_ix_k) = \mathrm{MIS}\left[p_{\mathrm{phase}}(\omega_i),p_{u_2}(\omega_i)\right]\ \mathrm{MIS}\left[p_{\mathrm{tr}}(t),p_{\mathrm{eq}}(t)\right]. \quad (7)$$

© 2016 The Author(s)
For personal use only. The definitive version is available at http://diglib.eg.org/.

Final Combination. When performing SNEE, we combine both subdivision strategies using MIS. The intermediate vertex x_j is thus drawn from a linear combination of both strategies, with the PDF computed as:

$$p(x_j|\mathbf{x}_i x_k) = \text{MIS}\left[p_{\downarrow}(x_j|\mathbf{x}_i x_k), p_{\uparrow}(x_j|\mathbf{x}_i x_k)\right]. \quad (8)$$

5. Integrating SNEE into Path Tracing

The variance of a forward path tracer is given by how successful it is in hitting the emitters (if all other terms can be importance sampled). Next-event estimation can significantly reduce the variance, but most NEE techniques, including SNEE, can synthesize only certain (multi-segment) connections. For instance, with the sampling of x_k described in Section 4.1, it cannot estimate light that refracts through boundary regions that are invisible to x_i (we discuss this in detail in Section 7). It is thus crucial that it can be easily incorporated into an algorithm that handles all the remaining transport; here we discuss the integration into a forward path tracer.

We use MIS to combine SNEE sampling strategies with strategies used in standard unidirectional path tracing. Whenever a complete light path is constructed, by either SNEE or forward tracing (with standard NEE), we evaluate the PDF of constructing the path using the other approach and compute the MIS weight. More precisely, for each SNEE connection, we compute the PDF for having generated the same subdivision sample using phase function and transmittance sampling in forward tracing. Analogously, once we cross the boundary with forward tracing, we compute the PDF of having generated the last two segments of that path using all techniques of SNEE (combined using MIS). The PDFs of both strategies are then used to compute the MIS weight.

6. Results

In order to assess the performance of path tracing with SNEE, we compare it against standard unidirectional path tracing which uses MIS of BSDF and light samples at x_k. We keep our test setup simple by using a single polygonal object bounding a homogeneous medium with a fixed albedo of 0.8 and an isotropic phase function. Figure 3 shows an *equal-sample-count* comparison at 500 samples per pixel (SPP) and contains only the light transport that can be handled by SNEE. Figure 4 shows an *equal-time* comparison at 30 s and contains all transport, including transport which is not handled by our technique, e.g. reduced radiance and single scattering. The left half of each image shows the result for standard unidirectional path tracing; the right half shows the result of incorporating our SNEE technique using MIS. In both figures we use a scattering medium with a low extinction coefficient of $2\,\text{m}^{-1}$ in the top row and a high extinction of $34\,\text{m}^{-1}$ for the bottom row; the height of the object is roughly 1 m.

We study the behavior of our technique over a wide range of different illumination and BSDF configurations. Each image triple within individual rows of Figures 3 and 4 uses one of three different lighting scenarios: an HDR environment light (importance sampled), a distant sphere light with a solid angle of 0.006 sr located above (note that this is 100 times larger than the solid angle of the Sun), and a delta directional light source. Within each triple, the BSDF varies from left to right: rough dielectric with a high roughness value of 0.2 (the width parameter of the GGX microfacet distribution), rough dielectric with a small roughness value of 0.04, and a smooth dielectric.

Our method always outperforms standard path tracing in the extreme case of illumination and BSDF both having a delta distribution (right-most columns in Figures 3 and 4). In this case the standard method will never be able to hit the directional light by sampling the BSDF and vice versa, therefore producing a black image. SNEE places vertices according to the incident light and is thus able to produce valid paths connecting the interior vertex to the emitter.

When the solid angle of the light, or the lobe of the BSDF, are finite, standard path tracing can form valid paths reaching the emitter. Its variance, however, is very high and using SNEE still provides tangible benefits. In cases when the surface has high roughness (nearly diffuse transmission), or the illumination is very low-frequency, the improvement of our method diminishes. This is to be expected as SNEE is designed to handle well difficult cases and its computational overhead may hurt performance in simple scenarios.

7. Discussion, Limitations, and Future Work

In this section, we discuss some of the limitations and challenges that we would like to address in the future.

Unhandled Light Transport. By only creating shadow connections at volume vertices, SNEE does not provide improvement for light transport that has a surface event at one of the last two bounces before exiting through the boundary: any path with suffix $\langle \mathbf{S}[\mathbf{S}|\mathbf{V}]\mathbf{SL}\rangle$, where **S**, **V**, and **L** represent surface, volume and light vertices, respectively. We handle these paths, e.g. single scattering, using standard unidirectional path sampling. The benefits of using SNEE for translucent objects dominated by low-order scattering thus diminish. Our initial tests of extending SNEE to single scattering revealed some challenges in designing good sampling densities. Namely, equiangular sampling, which assumes an isotropic directional distribution, can often lead to high variance. This could be mitigated by using an adaptive angular sampling [NNDJ12].

Perturbation NEE. One drawback of generating x_k, as described in Section 4.1, is that it considers only directly visible surfaces, and we thus have to rely on forward path tracing for transport that crosses the boundary at points *not visible* from x_i. An interesting alternative would be to generate the boundary vertex using a *two*-segment probe path, and then only *perturb* the middle vertex to satisfy the refraction constraint. Such construction, however, makes the evaluation of $p(x_k|\mathbf{x}_i)$ significantly more complicated; we need to marginalize over all possible two-segment paths that connect x_i and x_k. This is related to the problem that Hanika et al. [HDF15] sidestepped by assuming *bijection* between a seed path and the admissible path, i.e. the probe path and a perturbed path in our terminology, respectively. Unfortunately, we cannot employ analogous reasoning as any two-segment "seed" path can be mapped to any two-segment "admissible" path in our case.

© 2016 The Author(s)
For personal use only. The definitive version is available at http://diglib.eg.org/.

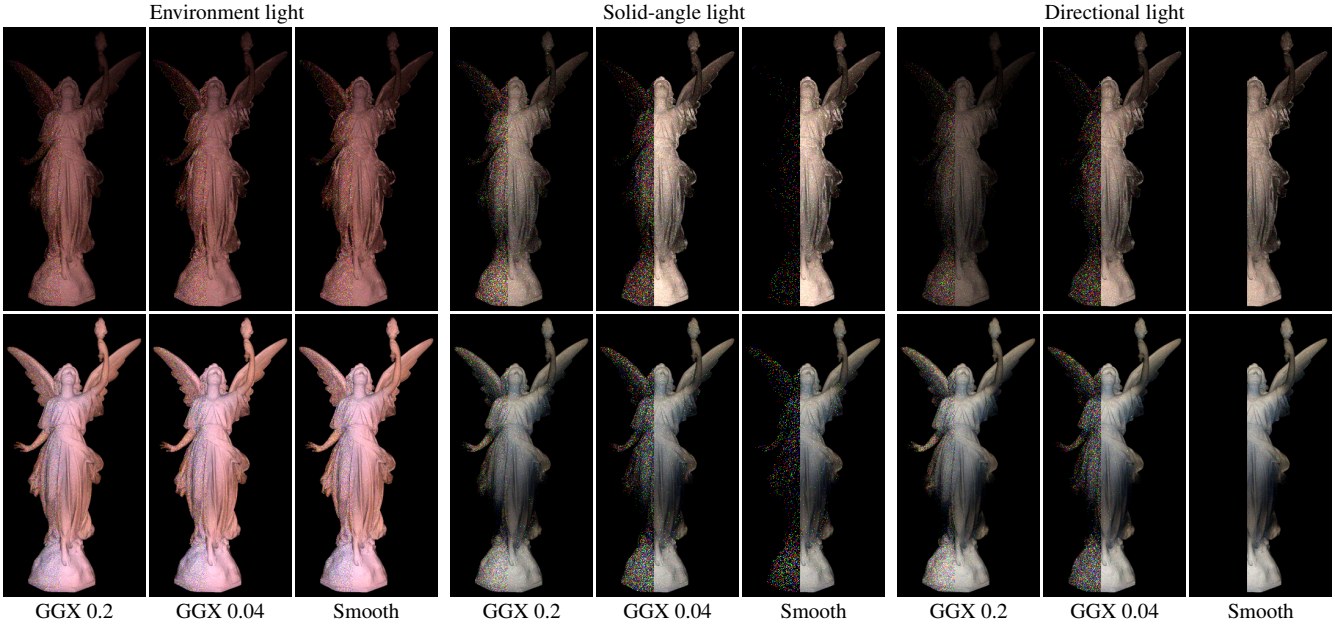

Figure 3: Equal-sample-count *comparison of standard unidirectional path tracing (left halves) against SNEE (right halves) showing only the transport that is handled by our technique. Sharpness of the BSDF lobe and illumination cone increases as we go from left to the right. Top row: low extinction. Bottom row: high extinction. See Section 6 for a detailed discussion.*

Computational Cost. While SNEE greatly reduces variance in the presence of highly directional, near-delta distributions, the benefits diminish when the boundary is rough, and lighting and phase functions become low-frequency. In such situations, equipping standard forward path tracing with SNEE can hurt performance due to the computational overhead of constructing the additional segments. We considered subdividing just the last segment of a fully constructed subsurface path to reduce the cost. The execution of NEE would then be conditioned on the probability of hitting the boundary vertex, which is difficult to compute, and thus prevents combining SNEE and forward path tracing using MIS. Reducing computational cost using a well-designed Russian roulette criterion, like Meng et al. [MPH*15], may be a more promising avenue to explore.

8. Conclusion

We proposed a new method for estimating incident light in participating media that arrives through a refractive boundary. Our subdivision next-event estimation handles cases where unidirectional path tracing struggles, or fails completely (objects with smooth dielectric boundaries illuminated by delta lights). We demonstrated the merit of using SNEE by comparing to the standard method. In many situations, especially the difficult ones, our approach yields significant benefits. We also discussed the remaining challenges that should be addressed to make SNEE fully practical.

Similarly to previous works, our technique is inspired by mutation and perturbation strategies found in the field of Metropolis light transport (MLT). We second the opinion that exploring these techniques within the context of basic MC rendering is a fruitful and promising avenue for future research.

© 2016 The Author(s)
For personal use only. The definitive version is available at http://diglib.eg.org/.

Acknowledgements

We thank reviewers for their valuable feedback and the Stanford Computer Graphics Laboratory for providing the 3D model of the Lucy statue.

References

[Cha60] CHANDRASEKHAR S.: *Radiative Transfer*. Dover Publications, 1960. 2

[Dwi82] DWIVEDI S.: A new importance biasing scheme for deep-penetration Monte Carlo. *Annals of Nuclear Energy 9*, 7 (1982), 359 – 368. 2

[GKH*13] GEORGIEV I., KŘIVÁNEK J., HACHISUKA T., NOWROUZEZAHRAI D., JAROSZ W.: Joint importance sampling of low-order volumetric scattering. *ACM TOG (Proc. of SIGGRAPH Asia) 32*, 6 (Nov. 2013), 164:1–164:14. 2, 3

[HDF15] HANIKA J., DROSKE M., FASCIONE L.: Manifold next event estimation. *CGF (Proc. of Eurographics Symposium on Rendering) 34*, 4 (2015), 87–97. 1, 2, 4

[HJ11] HACHISUKA T., JENSEN H. W.: Robust adaptive photon tracing using photon path visibility. *ACM TOG 30*, 5 (Oct. 2011), 114:1–114:11. 2

[Hol15] HOLZSCHUCH N.: Accurate computation of single scattering in participating media with refractive boundaries. *CGF (Proc. of Eurographics Symposium on Rendering) 34*, 6 (2015), 48–59. 1, 2

[ICG86] IMMEL D. S., COHEN M. F., GREENBERG D. P.: A radiosity method for non-diffuse environments. *Computer Graphics (Proc. of SIGGRAPH) 20*, 4 (Aug. 1986), 133–142. 1

[Jen96] JENSEN H. W.: Global illumination using photon maps. In *Proc. of Eurographics Workshop on Rendering Techniques* (London, UK, Aug. 1996), Springer-Verlag, pp. 21–30. 2

[JM12] JAKOB W., MARSCHNER S.: Manifold exploration: a Markov

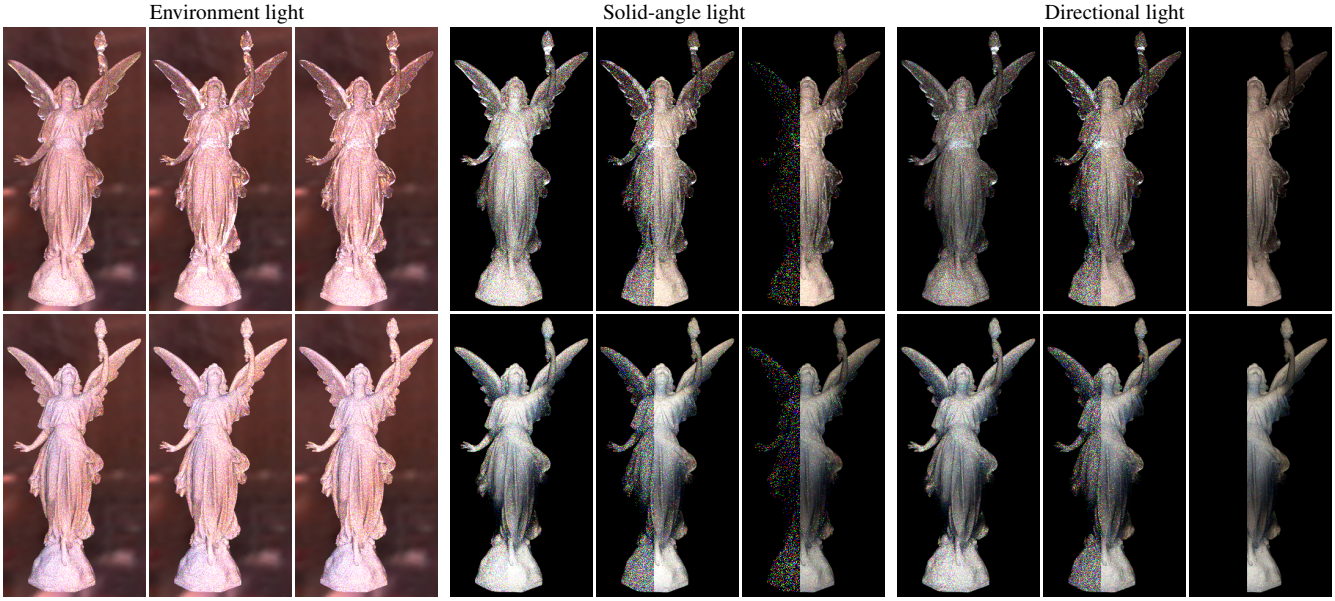

Figure 4: Equal-time *comparison of standard unidirectional path tracing (left halves) against SNEE (right halves) using the same setup as in Figure 3. Here we show all transport, including the transport which is not handled by our technique, such as single scattering. SNEE is designed to handle well the difficult cases and provides most benefits when the BSDF is narrow and the illumination high-frequency.*

Chain Monte Carlo technique for rendering scenes with difficult specular transport. *ACM TOG (Proc. of SIGGRAPH) 31*, 4 (July 2012), 58:1–58:13. 2

[JNSJ11] JAROSZ W., NOWROUZEZAHRAI D., SADEGHI I., JENSEN H. W.: A comprehensive theory of volumetric radiance estimation using photon points and beams. *ACM TOG 30*, 1 (Feb. 2011), 5:1–5:19. 2

[Kaj86] KAJIYA J. T.: The rendering equation. *Computer Graphics (Proc. of SIGGRAPH)* (1986), 143–150. 1

[Kal63] KALOS M. H.: On the estimation of flux at a point by Monte Carlo. *Nuclear Science and Engineering 16* (1963), 111–117. 2

[KC77] KALLI H., CASHWELL E.: *Evaluation of three Monte Carlo estimation schemes for flux at a point*. Tech. Rep. LA-6865-MS, Los Alamos Scientific Lab, New Mexico, USA, Sept. 1977. 2

[KD13] KAPLANYAN A. S., DACHSBACHER C.: Path space regularization for holistic and robust light transport. *Computer Graphics Forum (Proc. of Eurographics) 32*, 2 (2013), 63–72. 2

[Kd14] KŘIVÁNEK J., D'EON E.: A zero-variance-based sampling scheme for Monte Carlo subsurface scattering. In *ACM SIGGRAPH 2014 Talks* (New York, NY, USA, 2014), SIGGRAPH '14, ACM, pp. 66:1–66:1. 2

[KF12] KULLA C., FAJARDO M.: Importance sampling techniques for path tracing in participating media. *CGF (Proc. of Eurographics Symposium on Rendering) 31*, 4 (June 2012), 1519–1528. 2, 3

[LW93] LAFORTUNE E. P., WILLEMS Y. D.: Bi-directional path tracing. In *Compugraphics '93* (1993), pp. 145–153. 2

[MPH*15] MENG J., PAPAS M., HABEL R., DACHSBACHER C., MARSCHNER S., GROSS M., JAROSZ W.: Multi-scale modeling and rendering of granular materials. *ACM TOG (Proc. of SIGGRAPH) 34*, 4 (July 2015). 5

[NNDJ12] NOVÁK J., NOWROUZEZAHRAI D., DACHSBACHER C., JAROSZ W.: Progressive virtual beam lights. *CGF (Proc. of Eurographics Symposium on Rendering) 31*, 4 (June 2012), 1407–1413. 4

[PH10] PHARR M., HUMPHREYS G.: *Physically Based Rendering: From Theory to Implementation*, 2nd ed. Morgan Kaufmann Publishers Inc., San Francisco, CA, USA, 2010. 2

[RSK08] RAAB M., SEIBERT D., KELLER A.: Unbiased global illumination with participating media. In *Monte Carlo and Quasi-Monte Carlo Methods 2006*. Springer, 2008, pp. 591–606. 3

[RY94] REVUZ D., YOR M. J.: *Continuous martingales and Brownian motion*. Grundlehren der mathematischen Wissenschaften. Springer, Berlin, Heidelberg, 1994. 3

[SK71] STEINBERG H. A., KALOS M. H.: Bounded estimators for flux at a point in Monte Carlo. *Nuclear Science and Engineering 44* (1971), 406–412. 2

[SZLG10] SUN X., ZHOU K., LIN S., GUO B.: Line space gathering for single scattering in large scenes. *ACM TOG (Proc. of SIGGRAPH) 29*, 4 (July 2010), 54:1–54:8. 2

[VG94] VEACH E., GUIBAS L. J.: Bidirectional estimators for light transport. In *Proc. of Eurographics Rendering Workshop 1994* (1994), pp. 147–162. 2

[VG95] VEACH E., GUIBAS L.: Optimally combining sampling techniques for Monte Carlo rendering. In *Proc. of SIGGRAPH* (1995). 1

[VG97] VEACH E., GUIBAS L. J.: Metropolis light transport. In *Proc. of SIGGRAPH 97* (New York, NY, USA, 1997), Annual Conference Series, ACM Press/Addison-Wesley Publishing Co., pp. 65–76. 2

[VKv*14] VORBA J., KARLÍK O., ŠIK M., RITSCHEL T., KŘIVÁNEK J.: On-line learning of parametric mixture models for light transport simulation. *ACM TOG (Proc. of SIGGRAPH) 33*, 4 (July 2014), 101:1–101:11. 2

[WZHB09] WALTER B., ZHAO S., HOLZSCHUCH N., BALA K.: Single scattering in refractive media with triangle mesh boundaries. *ACM TOG (Proc. of SIGGRAPH) 28*, 3 (July 2009), 92:1–92:8. 1, 2

© 2016 The Author(s)
For personal use only. The definitive version is available at http://diglib.eg.org/.